

The interplay of VSCF/VCI calculations and matrix-isolation IR spectroscopy – Mid infrared spectrum of CH₃CH₂F and CD₃CD₂F

Dennis F. Dinu^{a,b,c}, Benjamin Ziegler^d, Maren Podewitz^a, Klaus R. Liedl^a, Thomas Loerting^b, Hinrich Grothe^c, Guntram Rauhut^{d,*}

^a Institute of General, Inorganic and Theoretical Chemistry, University of Innsbruck, Innrain 80-82, A-6020 Innsbruck, Austria

^b Institute of Physical Chemistry, University of Innsbruck, Innrain 52, A-6020 Innsbruck, Austria

^c Institute of Materials Chemistry, TU Wien, Getreidemarkt 9/BC/1, A-1060 Vienna, Austria

^d Institute of Theoretical Chemistry, University of Stuttgart, Pfaffenwaldring 55, D-70569 Stuttgart, Germany

ARTICLE INFO

Article history:

Received 22 September 2019

In revised form 5 November 2019

Accepted 5 November 2019

Available online 19 November 2019

ABSTRACT

We present the first matrix-isolation infrared (MI-IR) spectra of CH₃CH₂F and its isotopologue CD₃CD₂F in Neon and Argon matrix, together with new gas-phase IR spectra. Extensive vibrational self-consistent field and configuration interaction (VSCF/VCI) calculations are performed, based on an *ab initio* potential energy surface at ae-CCSD(T)-F12a/cc-pCVTZ-F12 level of electronic structure theory. We encounter an excellent agreement between VCI calculated transitions and the experimental MI-IR and gas-phase IR spectra. Mean absolute deviations are scattering between 1 and 4 cm⁻¹. The interplay of accurate vibrational structure calculations and high-resolution infrared experiments enables unprecedented insights in the CH respectively CD stretch region, providing the first rigorous assignment of the energetically very close ν_1 , ν_{12} and ν_{13} fundamental transitions.

© 2019 The Authors. Published by Elsevier Inc. This is an open access article under the CC BY license (<http://creativecommons.org/licenses/by/4.0/>).

1. Introduction

With the Montreal protocol from 1987 and its following Amendments [1], there exists an international agreement on banning specific halogenated hydrocarbons for the use as refrigerants, propellants or solvents, among others. Initially, this agreement dealt with chlorofluorocarbons (CFC) and their partially hydrated derivatives, as they possess a high ozone depletion potential (ODP). While the ban successfully reduced the emission of CFCs, increasing concentration of chlorine free alternatives with low ODP can be observed in the atmosphere [2]. The latter species were initially not addressed by the Montreal protocol, just to mention the hydrofluorocarbon HFC-134a (or CH₂FCF₃) [3,4]. Unfortunately, HFCs can possess a high global warming potential (GWP) and can be considered as greenhouse gases. Those substances were partially addressed in 1997 by the Kyoto protocol, which aims at substances that accelerate the greenhouse effect [5]. For HFC species such as fluoroform, or HFC-23, bans are not recommendable. Such HFCs have an important function as fire extinguishing agents and if used for this purpose only their emission into atmosphere is limited. More intriguing is the use of HFCs as alternative

refrigerants. The research for reasonably priced alternatives has shown to be of outstanding importance, especially for highly-populated developing countries [6]. Mixtures of hydrocarbons and HFCs have been considered due to their promising characteristics of zero ODP and low GWP. Fluoroethane (CH₃CH₂F), also known as HFC-161, is mentioned as an important ingredient in refrigerant mixtures that are promising alternative candidates to previously used CFC-502 (widely known as Freon) or to other refrigerant mixtures [7,8]. The increasing use of HFCs in alternative refrigerants is evident, as their ban by the Montreal protocol is projected into the far future. Only in 2016, the Kigali Amendment specifically set the goal to reduce the use of HFCs until 2047 [1]. Today, the greenhouse gas most focused on is CO₂, which is strongly underpinned by the 2018 special report on global warming by the IPCC [9]. Thus, the monitoring of hydrocarbon and HFC mixtures as potential greenhouse gases in the atmosphere may seem secondary. However, with the commercial availability of such mixtures as refrigerants and their massive use in developing countries, further increasing emissions of HFCs into the atmosphere cannot be ruled out.

The monitoring of HFCs, such as fluoroethane, can be accomplished by infrared (IR) spectroscopy. However, the vibrational structure of hydrocarbons is inherently involved, as the fundamental CH stretch vibration partially overlaps with combination bands and overtones of the CH deformation. Resonances additionally

* Corresponding author.

E-mail addresses: dennis.dinu@uibk.ac.at (D.F. Dinu), rauhut@theochem.uni-stuttgart.de (G. Rauhut).

complicate the situation and covalently bound halogen atoms introduce frequency shifts in both the CH stretch and deformation modes. In gas-phase IR spectroscopy, the spectrum is further complicated by rotational-vibrational fine structure. All this is reflected in the rather limited amount of literature data available for such species as fluoroethane. Two early assignments of its gas-phase IR and Raman spectrum are dating back to 1952 by Smith et al. [10] and to 1972 by Shimanouchi [11]. While Shimanouchi somewhat fails to uniquely assign the spectral region around the CH stretch vibrations or only with significant uncertainties, Smith et al. provides a consequent assignment. The latter is based on a series of gas-phase and liquid IR/Raman experiments on fluorinated ethane species. However, it lacks a rigorous theoretical model of the ethane and relies on analogous assignments of methane species. In 1975, elucidation of the CH stretch region was partially improved by further extensive experimental effort [12], as summed up by McKean et al. [13], still without a conclusive assignment for all fundamentals. An unambiguous spectral assignment is possible when highly accurate predictions based on a reliable theoretical model are considered. With calculations based on the harmonic approximation (HA), a broad prediction of frequencies and structural parameters for various fluoroethane species was provided in 1996 by Papisavva et al. [14]. To overcome the intrinsic overestimation of frequencies by the HA, McKean [15,16] derived various scaling factors. Only this effort allowed McKean to improve the assignment for the fundamental vibrations relying on an harmonic treatment of fluoroethane [16].

However, the required computational accuracy to resolve the vibrational structure of the CH region cannot be achieved within a simplified theoretical model, such as the HA. In view of accuracy, an exact model for the vibrational structure of the specific hydrofluorocarbon is desirable, yet, some level of approximation must be maintained if the approach should be flexible to be used also for other hydrocarbons than the one at hand. To strike a balance between accuracy and flexibility, we here employ the approach of vibrational self-consistent field (VSCF) and vibrational configuration interaction (VCI) theory, based on a multi-mode potential energy surface (PES) at ae-CCSD(T)-F12a/cc-pCVTZ-F12 level of electronic structure theory. With this entirely *ab initio* approach that inherently incorporates anharmonicity, we tackle the spectroscopic characterization of halogenated hydrocarbons, at the specific example of fluoroethane CH₃CH₂F. Consequently, we provide the first extensive VSCF/VCI calculations for this type of hydrofluorocarbon. At the same time we perform new IR experiments, where the most prominent issue in gas-phase IR spectra is band-broadening by rotational-vibrational fine splitting. We decided to overcome this issue by matrix-isolation infrared (MI-IR) spectroscopy, which inhibits rotation and, hence, yields pure vibrational spectra. We recorded MI-IR spectra of fluoroethane (CH₃CH₂F and CD₃CD₂F) in solid Argon and Neon and, for validation, a simple gas-phase IR spectrum.

2. Experimental details

Pure samples of CH₃CH₂F (ethyl fluoride 97%, CAS: 353-36-6, Apollo Scientific UK, Code: PC3206, Lot: AS446839) and CD₃CD₂F (ethyl fluoride-d5 99.6%, CAS: 53886-01-4, CDN Isotopes Canada, Code: D-6675, Lot: V-620) were used for all matrix-isolation and gas-phase experiments. For MI-IR, the samples were diluted each in Neon and Argon. The dilution was adjusted in a mixing chamber with a reservoir of approx. 2 L volume, previously evacuated to 10⁻⁵ mbar. A dilution of 1:1000 denotes a mixture of 1 mbar sample and roughly 1000 mbar of rare gas. Mixtures of 1:250, 1:1000, 1:2000 and 1:8000 in Neon and 1:1000, 1:2000 and 1:8000 in Argon were prepared. From the reservoir, a part of the mixture

gas was transferred with a rate of 8 mbar/min for 30 min into a cryostat, which was constantly evacuated to 10⁻⁷ mbar and cooled to 5.8 K during this procedure. On a gold plate within the cryostat, the gas mixture was deposited as a solid matrix at 5.8 K. The apparatus is explained in more detail elsewhere [17,18]. Gas-phase spectra were obtained by transferring roughly 20 mbar of the pure sample gas (no mixture with Ar or Ne) into the cryostat at room temperature. For both gas-phase and matrix-isolation, FTIR spectra were recorded with 512 scans and a resolution of 0.3 cm⁻¹ in the region of 7500–500 cm⁻¹ using the FTIR spectrometer Vertex 80v (Bruker, Karlsruhe). Additionally, a spectrum of solid CH₃CH₂F at 5.8 K was recorded.

3. Computational details

The equilibrium structure and harmonic frequencies of CH₃CH₂F have been determined at two different levels of electronic structure theory, namely explicitly correlated coupled-cluster theory [19], CCSD(T)-F12a, within the frozen core (fc) approximation and with the explicit consideration of core-correlation effects, *i.e.*, all electron (ae) calculations. Within the latter type of calculations, different exponents γ were used for the Slater geminal functions referring to core-core, core-valence, and valence-valence orbital pairs, *i.e.*, 0.8, 1.7 and 2.2 as recommended by Werner et al. [20]. For the frozen core calculations a constant γ of 1.0 has been chosen. Moreover, a cc-pVTZ-F12 basis has been used for the fc-CCSD(T)-F12 calculations, while a cc-pCVTZ-F12 has been employed in the ae-CCSD(T)-F12 calculations [21]. As explicitly correlated coupled-cluster calculations converge much faster with respect to the size of the basis set than conventional coupled-cluster calculations, our results can roughly be compared with conventional CCSD(T) calculations in combination with a quintuple- ζ basis set [22]. It is well-known that the explicit account of core-correlation effects leads to an upshift of the vibrational frequencies, which often results in an overestimation of the transition energies. This upshift usually is partly canceled by high-order coupled-cluster terms, *e.g.* quadruple excitations in the coupled-cluster expansion [23–25]. However, CCSDT(Q) calculations were not feasible for this rather large system and thus our ae-CCSD(T)-F12a frequencies are expected to be slightly too high. On the other hand, the fc-CCSD(T)-F12a frequencies apparently rely on error compensation, which is unsatisfying once high accuracy is aimed at. In any case, we found that core-correlation effects might be important for an improved description of the CH-stretching modes and thus we present both, fc and ae calculations.

The equilibrium structure was taken as an expansion point of an *n*-mode expansion [26] of the potential energy surface (PES), which has been truncated after the 4-mode coupling terms. For that, canonical normal coordinates were used [27]. Due to the low symmetry of the molecule, this resulted in slightly more than 10⁶ *ab initio* single point calculations, which have been distributed among 128 cores. This number sounds very large, but essentially it corresponds on average to just 4.2 *ab initio* calculations in each direction of the 3060 4-mode coupling terms. In order to limit the computational effort, a multi-level approximation [28,29] has been used, in which the 1-mode and 2-mode coupling terms have been determined at the CCSD(T)-F12a/cc-p(C)VTZ-F12 level, while a smaller basis set of cc-p(C)VDZ-F12 quality has been used for the 3-mode and 4-mode couplings. Efficient Kronecker product fitting has been used to transform the potential in an analytical sum-of-products representation of 8 polynomials in each direction [30].

Vibrational self-consistent field (VSCF) theory employing 20 mode-specific distributed Gaussians has been used to determine a modal basis for subsequent configuration-selective vibrational configuration interaction (VCI) calculations [31–33]. The initial

correlation space within these calculations comprised quintuple excitations and resulted in $1.7 \cdot 10^7$ configurations, from which the most important ones have been identified on the basis of a perturbational selection criterion. All VCI calculations were based on modals being optimized for the vibrational ground state. For the calculations of combination bands an even larger correlation space including 6-tuple excitation ($8.6 \cdot 10^7$ initial configurations) has been used. Vibrational angular momentum terms have been included using the approximation of a constant μ -tensor [34]. Note that the VCI matrix has been stored in sparse matrix format and an iterative residuum based eigenvalue solver has been used to enable these large calculations [35].

4. Results and discussion

4.1. Geometrical parameters and rotational constants

In a first step we have computed the geometrical parameters and rotational constants of fluoroethane and its d_5 -isotopologue. Its structure and the labeling of the atoms are displayed in Fig. 1. In Table 1 we have listed the equilibrium geometrical parameters for fluoroethane obtained from ae-CCSD(T)-F12a/cc-pCVTZ-F12

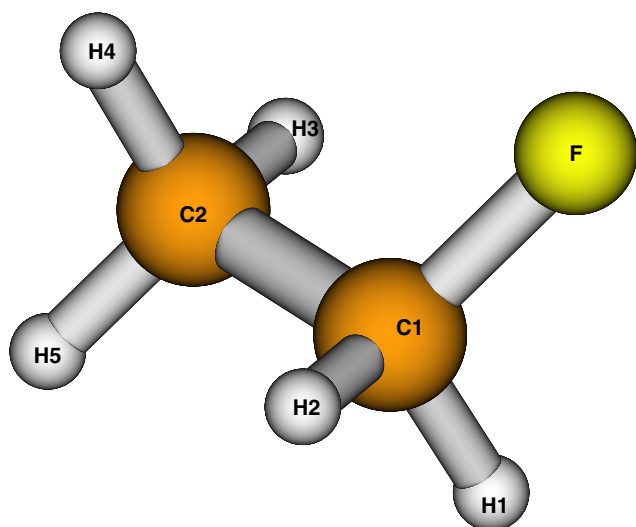


Fig. 1. Geometry and atom labeling of fluoroethane.

calculations and compare them in the case of $\text{CH}_3\text{CH}_2\text{F}$ with experimental data obtained from electron diffraction (ED) or microwave (MW) measurements [36,37]. For $\text{CD}_3\text{CD}_2\text{F}$, no experimental reference data were found, hence, the computational results for this isotopologue can be seen as a prediction.

Equilibrium geometrical parameters r_e are obtained from geometry optimization within the Born-Oppenheimer approximation. Vibrational effects obtained from VCI calculations for the vibrational ground-state have been accounted for, following two different routes. While r_g parameters represent an average value of an instantaneous inter-nuclear distance and have been calculated from a VCI expectation value of the bond lengths expanded in terms of normal coordinates, r_a distances have been determined from zero-point averaged atomic positions. Typically, r_g and r_a values differ quite substantially as is confirmed by the values listed in Table 1. In general, our vibrationally averaged r_a values obtained from ae-CCSD(T)-F12a/cc-pCVTZ-F12 calculations agree very nicely with the microwave data of Nygaard from 1966. The agreement with our frozen core calculations is slightly worse and therefore we focus primarily on the all electron results. However, for the C_1C_2 bond length and the FC_1H_1 angle the agreement is not as good as for the other parameters. Our $r_a(\text{C}_1\text{C}_2)$ bond length (1.5146 Å) is markedly longer than obtained from MW measurements (1.505 Å). Interestingly, Beagley et al. determined this bond lengths in ED measurements to be much longer (1.512 Å), but found a strong dependence on refinement procedures, which they applied within their determination.

For calculating vibrationally averaged rotational constants, we have employed a hybrid approach, in which the expectation value of the μ -tensor [38], as occurring in the Watson-Hamiltonian [39], has been augmented by the Coriolis coupling term as arising in 2nd order vibrational perturbation theory, cf. Eq. (1).

$$B_v^x \approx \frac{\langle \mu_{xx} \rangle_v}{2} + \sum_k \frac{2B_e^x}{\omega_k} \sum_l \frac{(\zeta_{kl}^x)^2 (3\omega_k^2 + \omega_l^2)}{\omega_k^2 - \omega_l^2} \left(v_k + \frac{1}{2} \right) \quad (1)$$

It has been shown for several molecules that this approximation yields reliable results [40].

Table 2 lists results obtained from frozen-core calculations and from all-electron calculations as well as experimental results from the literature [36]. The pronounced differences between the ae and fc calculations showing up for the rotational constants, indicate that core-correlation effects are quite important for this molecule. Our all-electron calculations are in markedly better agreement with the experimental results of Nygaard than the frozen core calculations. Consequently, we expect our all-electron calculations for

Table 1

Computed geometrical parameters (ae-CCSD(T)-F12a/cc-pCVTZ-F12) of $\text{CH}_3\text{CH}_2\text{F}$ and $\text{CD}_3\text{CD}_2\text{F}$. Bond lengths are given in Å, angles in degree.

Parameter ^a	$\text{CH}_3\text{CH}_2\text{F}$					$\text{CD}_3\text{CD}_2\text{F}$	
	Exp. ^b		Calc. ^c			r_a	r_g
	ED	MW	r_e	r_a	r_g		
$r(\text{C}_1\text{C}_2)$	1.512	1.505	1.5055	1.5146	1.5158	1.5137	1.5151
$r(\text{C}_1\text{F})$	1.396	1.398	1.3906	1.3971	1.3986	1.3967	1.3986
$r(\text{C}_1\text{H}_1)$	1.102	1.098	1.0893	1.0990	1.1116	1.0964	1.1055
$r(\text{C}_2\text{H}_3)$	1.102	1.090	1.0879	1.0906	1.1094	1.0906	1.1036
$r(\text{C}_2\text{H}_5)$	1.102	1.091	1.0897	1.0903	1.1112	1.0910	1.1055
$\angle(\text{C}_2\text{C}_1\text{F})$	109.7	109.7	109.64	109.59		109.60	
$\angle(\text{FC}_1\text{H}_1)$	106.1	106.1	107.22	107.22		107.19	
$\angle(\text{H}_1\text{C}_1\text{H}_2)$	109.0	108.8	109.04	108.95		109.03	
$\angle(\text{H}_3\text{C}_2\text{C}_1)$	112.9		110.52	110.73		110.65	
$\angle(\text{H}_5\text{C}_2\text{C}_1)$	109.7	109.7	109.77	109.86		109.79	
$\angle(\text{H}_3\text{C}_2\text{H}_4)$	109.0	108.9	108.81	108.58		108.66	
$\tau(\text{H}_2\text{C}_1\text{C}_2\text{H}_4)$			58.50	58.51		58.46	

^a For the labeling of the atoms see Fig. 1.

^b Electron diffraction (ED) data (refinement I) taken from Ref. [37]. Microwave (MW) data taken from Ref. [36].

^c Geometry parameters without (r_e) and including vibrational effects (r_g , r_a), see text.

Table 2

Computed rotational constants (B_e) and ground-state vibrationally averaged rotational constants (B_0) of $\text{CH}_3\text{CH}_2\text{F}$ and $\text{CD}_3\text{CD}_2\text{F}$. All values are given in GHz.

	$\text{CH}_3\text{CH}_2\text{F}$			$\text{CD}_3\text{CD}_2\text{F}$	
	Exp. ^a	Calc. (fc)	Calc. (ae)	Calc. (fc)	Calc. (ae)
A_e		36.32357	36.46517	23.32094	23.40537
B_e		9.41529	9.44529	7.80682	7.83177
C_e		8.25216	8.27966	6.85532	6.87792
A_0	36.07050	35.92502	36.06533	23.09803	23.18154
B_0	9.36460	9.33365	9.36336	7.74252	7.76740
C_0	8.19978	8.17196	8.19915	6.79449	6.81698

^a Experimental data taken from Ref. [36].

the rotational constants of the penta-deuterated species, for which experimental results are not available, to be the most accurate prediction.

4.2. Comparison of fundamental vibrational transitions in gas-phase IR, MI-IR and VCI computation

All experimentally observed bands in the Neon and Argon MI-IR as well as gas-phase IR spectra are documented in the [Supplementary Information](#). To aid the discussion, a restricted representation of the CH resp. CD stretch regions of those spectra are depicted in [Fig. 2](#) for $\text{CH}_3\text{CH}_2\text{F}$ resp. in [Fig. 3](#) for $\text{CD}_3\text{CD}_2\text{F}$. Some general characteristics can be noticed for both species. In the Ne MI-IR experiment with the lowest sample dilution (1:250), some bands exhibit a splitting that is accompanied with band broadening. This effect is most likely due to oligomerization and can be impeded when going to higher sample dilution (1:1000, etc.). In the highest diluted mixtures, however, splittings of roughly 0.5 to 3 cm^{-1} remain. These are more pronounced in the Ne MI-IR spectrum, yet, also occur partially in the Ar MI-IR spectrum. We assume that the fluoroethane can visit different matrix trapping sites, created by the insertion

of fluoroethane molecules into gaps within the noble gas matrix or by the substitution of one or more noble gas atoms with the fluoroethane. The structural distortion of the so trapped molecule results in small vibrational frequency shifts, which appear as band splitting in the spectra. We do not observe a correlation between the matrix splitting for $\text{CH}_3\text{CH}_2\text{F}$ and for $\text{CD}_3\text{CD}_2\text{F}$ in the whole spectrum, yet, there are some similarities, e.g., in the CH resp. CD stretch region.

In addition to the matrix splittings, we observe overall shifts of the vibrational frequencies in the matrix environment compared to gas-phase. To provide some values for these matrix shifts, we here use in advance our assignment of fundamental vibrational transitions. As must be expected, the Ar MI-IR spectra exhibit slightly stronger matrix shifts than the Ne MI-IR spectra. Considering the fundamental vibrational transitions of $\text{CH}_3\text{CH}_2\text{F}$, the Ar MI-IR data in comparison to gas-phase IR data shows a mean absolute deviation (MAD) of 4 cm^{-1} and a maximum deviation (MAX) of 8.1 cm^{-1} . Ne MI-IR data compared to gas-phase data shows a MAD of 1 cm^{-1} (MAX = 2.7 cm^{-1}). Similar matrix shifts are observed for the $\text{CD}_3\text{CD}_2\text{F}$, where the Ar MI-IR data shows a MAD of 4.0 cm^{-1} (MAX = 7.6 cm^{-1}) and the Ne MI-IR data shows a

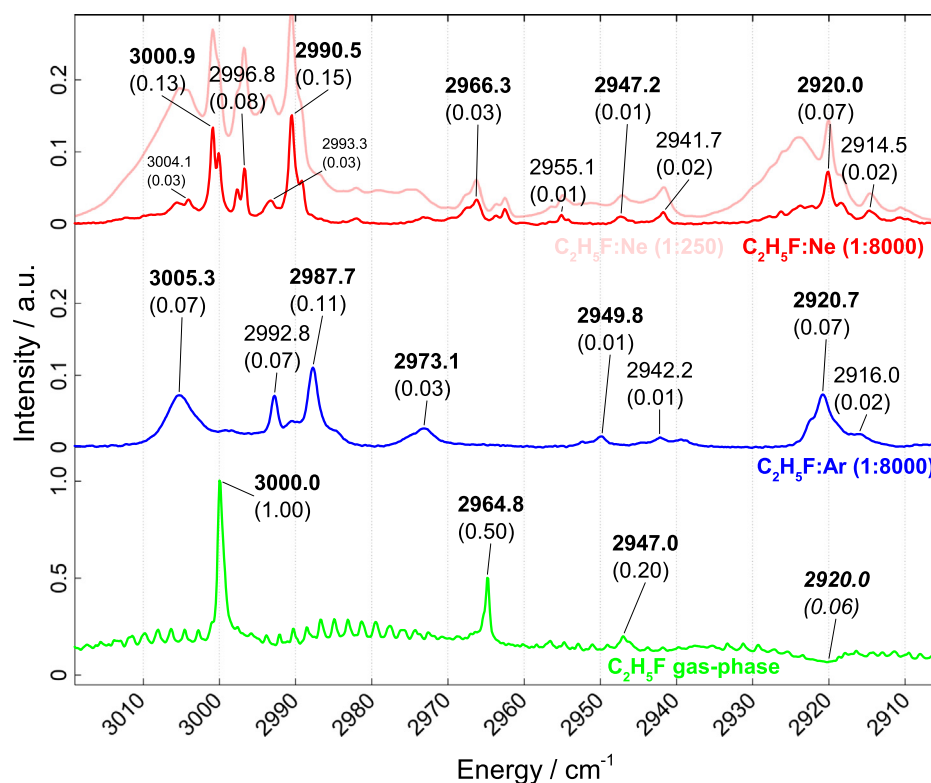


Fig. 2. Fluoroethane $\text{CH}_3\text{CH}_2\text{F}$. Experimental Ne MI-IR (red) and Ar MI-IR (blue) at 6 K, and gas-phase IR spectrum (green) at 273 K. Spectral region of the fundamental CH stretch vibrations. Assigned fundamental vibrational transitions are highlighted in bold and indirectly observed transitions highlighted in italics. (For interpretation of the references to colour in this figure legend, the reader is referred to the web version of this article.)

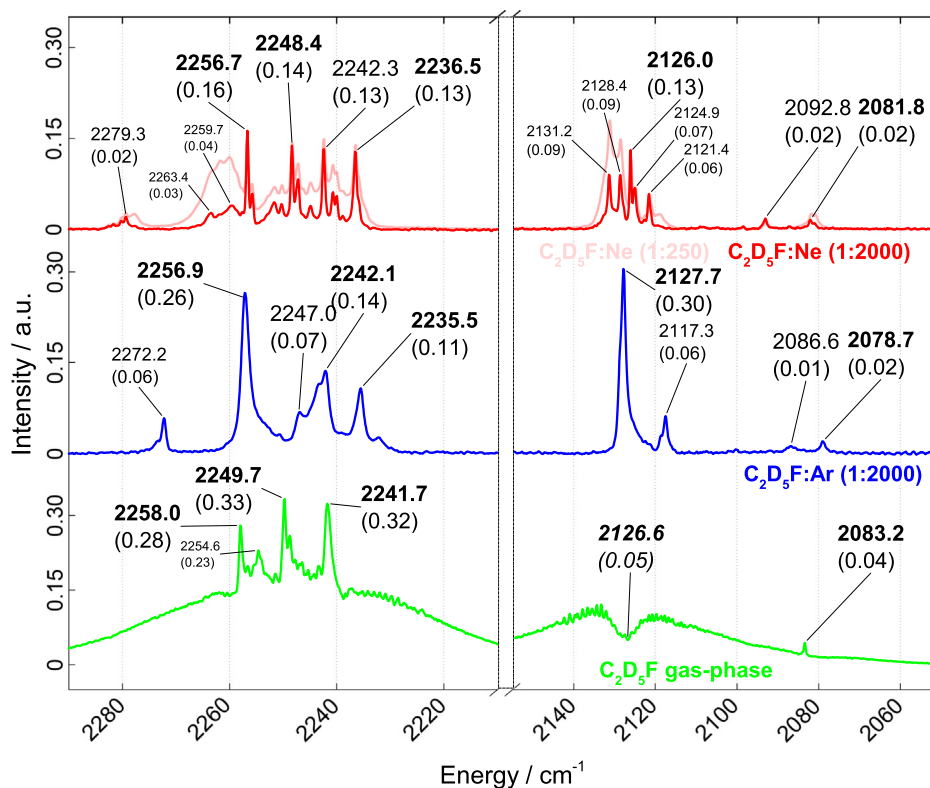


Fig. 3. Fluoroethane- d_5 CD_3CD_2F . Experimental Ne MI-IR (red) and Ar MI-IR (blue) at 6 K, and gas-phase IR spectrum (green) at 273 K. Spectral region of the fundamental CH stretch vibrations. Assigned fundamental vibrational transitions are highlighted in bold and indirectly observed transitions are highlighted in italics. (For interpretation of the references to colour in this figure legend, the reader is referred to the web version of this article.)

MAD of 2.0 cm^{-1} (MAX = 5.2 cm^{-1}), both compared to gas-phase IR data. This difference in the matrix shifts, of course, manifests itself in the deviation between VCI calculation and MI-IR experiment. Considering again the fundamental vibrational transitions of CH_3CH_2F , the calculated VCI(ae) data is in very good agreement with gas-phase IR data (MAD = 3 cm^{-1} , MAX = 9 cm^{-1}) as well as Ne MI-IR data (MAD = 2.1 cm^{-1} , MAX = 7.4 cm^{-1}) and agrees slightly worse with the Ar MI-IR observations (MAD = 4.1 cm^{-1} , MAX = 12.5 cm^{-1}). Also for CD_3CD_2F , the calculated VCI(ae) data compares very good with gas-phase IR data (MAD = 2.1 cm^{-1} , MAX = 2.2 cm^{-1}) and Ne MI-IR data (MAD = 2.7 cm^{-1} , MAX = 5.4 cm^{-1}) and slightly worse with Ar MI-IR data (MAD = 4.6 cm^{-1} , MAX = 8.9 cm^{-1}). The higher MAX and MAD in the Ar MI-IR data indicate a more pronounced interaction of fluoroethane with the Argon environment than with the Neon environment. As the VCI calculations are based on a model of fluoroethane *in vacuo*, it is desirable that the calculations represent the gas-phase observations best. Nevertheless, the close agreement between VCI calculations and Ne MI-IR affirms the choice of this type of experiment.

Gas-phase IR spectra, however, have not been assigned unambiguously in the past. The main problem, which we also encounter in our gas-phase IR experiments, is the rotational-vibrational fine structure that envelops the non-rotating transitions. In some regions, the P- and R-branches are so pronounced, that the non-rotating transitions can only be observed indirectly (cf. 2920 cm^{-1} in Fig. 2 or 2126.6 cm^{-1} in Fig. 3). Hence, for some vibrational transitions only a crude estimation can be given in gas-phase IR spectra, while Ne or Ar MI-IR spectra the assignment is less problematic. While Smith et al. [10] managed to give a conclusive characterization, Shimanouchi [11] reported some inconclusive assignments in the spectral region between 3010 cm^{-1} and 2910 cm^{-1} for CH_3CH_2F . A closer look at the literature data

reveals some inconsistencies, which we resolve by a close combination of MI-IR spectra and VCI calculations in the process of assignment. In both gas-phase IR and MI-IR, we are in a position to provide a rigorous assignment for all fundamental vibrational transitions and some overtones and combination bands. Our assignment is discussed in the following two subsections independently for CH_3CH_2F and CD_3CD_2F , and documented together with the computed vibrational frequencies in Table 3 for CH_3CH_2F and in Table 5 for CD_3CD_2F . It is comparable to the assignment employed by McKean [16] to interpret his HA calculations. In the last subsection, we report and discuss isotopic frequency shifts from experiment and theory.

4.3. Assignment of the fundamental vibrational transitions in the gas-phase and MI-IR spectrum of CH_3CH_2F

The region of the spectrum up to 1500 cm^{-1} is dominated by isolated fundamental transitions, which can undoubtedly be assigned. Both, Smith et al. [10] and Shimanouchi [11], observe a fundamental band at 1479 cm^{-1} , which is assigned by Shimanouchi as the ν_4 transition with a $3\text{--}6\text{ cm}^{-1}$ uncertainty. Despite its rotational-vibrational fine splitting, we do not directly observe the band corresponding to the fundamental vibration in our gas-phase IR spectrum. Still we can estimate the non-rotating transition to be centered in between the P- and R-branches at around 1491 cm^{-1} . In Ne MI-IR we observe a band at 1489.0 cm^{-1} , which is in good agreement with the VCI computed ν_4 transition (1491.4 cm^{-1}). Note that Shimanouchi assigns the two transitions (ν_5 and ν_{14}) to one band at 1449 cm^{-1} with an error bar of $6\text{--}15\text{ cm}^{-1}$. Smith et al. report two not uniquely assigned fundamentals at 1449 cm^{-1} and 1456 cm^{-1} . This is not necessarily supported by our results. On the one hand, we directly observe the band at 1449 cm^{-1} in our gas-phase IR

Table 3
Experimental and computed vibrational frequencies of CH₃CH₂F. All quantities are given in cm⁻¹.

Mode	Sym.	Experiment ^a			Calculation ^b				
		Gas	Ne	Ar	Harm.	VCI(fc)	$\Delta\nu_i$ (fc)	VCI(ae)	$\Delta\nu_i$ (ae)
ν_1 ^g	A'	2985 ^d	2990.5	2987.7	3060.1	2983.5	-7.0/4.2	2990.2	-0.3/2.5
ν_2	A'	2947	2947.2	2949.9	3046.1	2942.6	4/4.6/7.3	2948.7	2/1.5/1.2
ν_3	A'	2920	2920.0	2920.7	3002.9	2918.3	2/1.7/2.4	2925.4	5/5.4/4.7
ν_4	A'	1491	1489.0	1485.6	1530.2	1488.3	3/0.7/2.7	1491.4	0/2.4/5.8
ν_5	A'	1466	1464.3	1461.1	1507.4	1462.4	4/1.9/1.3	1465.1	1/0.8/4.0
ν_6	A'	1397	1397.4	1395.0	1432.0	1395.7	1/1.7/0.7	1398.8	2/1.4/3.8
ν_7	A'	1365 ^e	1371.3	1369.2	1402.5	1368.5	-2.8/0.7	1372.0	-0.7/2.8
ν_8	A'	1109	1108.6	1105.1	1132.2	1106.9	2/1.7/1.8	1110.1	1/1.5/5.0
ν_9	A'	1050	1051.4	1046.3	1084.5	1055.4	5/4.0/9.1	1058.8	9/7.4/12.5
ν_{10}	A'	881	879.0	874.5	895.4	878.1	3/0.9/3.6	880.7	0/1.7/6.2
ν_{11}	A'	415 ^f	n.o. ^c	n.o. ^c	411.3	411.0		413.1	
ν_{12}	A''	3000	3000.9	3005.3	3141.3	2993.4	7/7.5/11.9	3000.7	1/0.2/4.6
ν_{13}	A''	2965	2966.3	2973.1	3104.3	2962.8	2/3.5/10.3	2969.5	5/3.2/3.6
ν_{14}	A''	1449	1448.1	1444.7	1489.1	1445.0	4/3.1/0.3	1447.3	2/0.8/2.6
ν_{15}	A''	1274	1276.7	1276.8	1307.6	1275.0	1/1.7/1.8	1278.8	5/2.1/2.0
ν_{16}	A''	1172	1172.9	1171.0	1195.7	1171.6	0/1.3/0.6	1174.5	3/1.6/3.5
ν_{17}	A''	810	811.0	807.7	811.9	805.7	4/5.3/2.0	808.9	1/2.1/1.2
ν_{18}	A''	243 ^e	n.o. ^c	n.o. ^c	251.5	248.6		249.0	
						MAD	3/3.1/3.8		3/2.1/4.1
						MAX	7/7.5/11.9		9/7.4/12.5
$2\nu_4$ ^g	A'		2996.8	2992.8	3126.3	2988.6		2995.0	
$2\nu_5$	A'		2914.5	2916.0	3014.7	2908.3		2913.8	
$2\nu_{14}$	A'	2882	2879.0	2873.4	2978.2	2875.6		2880.7	
$2\nu_6$	A'		2781.3	2777.0	2864.0	2778.9		2782.2	
$\nu_5 + \nu_6$	A'		2856.0	2851.0	2939.3	2851.5		2857.2	
$\nu_5 + \nu_7$	A'	2831	2830.0	2825.0	2909.8	2823.2		2829.3	
$\nu_6 + \nu_7$	A'	2751	2749.6	2746.6	2823.4	2743.5		2749.7	
$\nu_{14} + \nu_{15}$	A'		2731.1	2726.4					
$\nu_{17} + \nu_{18}$	A'		1070.5	1071.0	1063.4	1065.2		1068.7	

^a Vibrational frequencies measured in gas-phase, Ne matrix and Ar Matrix, this work.

^b Harmonic frequencies from fc-CCSD(T)-F12a/cc-pVTZ-F12 calculations. Anharmonic frequencies from VCI calculations including up to quintuple excitations, relying on a PES based on the frozen core (fc) approximation resp. on all electron (ae) correlation. Deviations $\Delta\nu_i$ of the VCI(fc) and VCI(ae) frequencies calculated w.r.t. experimental Gas/Ne/Ar data.

^c Not observed, as the frequency is below the experimental spectral range.

^d Taken from gas-phase reference [12]. Observation questionable, see text.

^e Taken from gas-phase reference [11].

^f Taken from gas-phase reference [10].

^g Strong Fermi resonance, see text and Table 4.

experiment, yet, in the MI-IR experiments we observe two well separated bands at 1464 cm⁻¹ (ν_5 , Ne matrix) and 1448 cm⁻¹ (ν_{14} , Ne matrix), which agree nicely with our VCI calculations. Similar to the ν_4 transition, we can estimate the ν_5 transition in our gas-phase IR experiment at roughly 1466 cm⁻¹. In gas-phase literature data, a fundamental transition is observed at 1395 cm⁻¹ and assigned as ν_6 with an uncertainty of 3–6 cm⁻¹ by Shimanouchi. In our gas-phase experiment, we observe a triply split band, with the most intense peak at 1397.4 cm⁻¹, which agrees well with VCI and Ne MI-IR. The ν_7 transition is not observed in our gas-phase IR spectrum. This fits to the very low intensity of this transition predicted by our calculations. However, weak bands are visible in MI-IR (1371.3 cm⁻¹, Ne matrix). While Smith et al. observe a fundamental transition at 1365 cm⁻¹ in liquid-phase, Shimanouchi also reports the same band with an error bar of 6–15 cm⁻¹ in the gas-phase. We cannot provide a better estimation for the gas-phase, yet, it is safe to assume that the literature assignment is not ideal at this point. Despite the low intensity, we observe the ν_{15} transition in gas-phase IR at 1274.4 cm⁻¹, which is slightly lower than reported in literature at 1277 cm⁻¹. In the Ne and Ar MI-IR experiments it is only observed at very low dilution. Shimanouchi and Smith et al. assign a band at 1048 cm⁻¹ to a A' fundamental, strictly speaking the ν_{16} transition. We consider this a misassignment, as we observe this transition at 1172.8 cm⁻¹ in gas-phase IR and at 1172.9 cm⁻¹ in Ne MI-IR, both in perfect agreement with the VCI calculated ν_{16} transition of A'' symmetry. In fact, Smith et al. assign a band at 1171 cm⁻¹ to a A' fundamental. The ν_8

transition is observed in MI-IR (1108.6 cm⁻¹, Ne matrix) and can be indirectly deduced at 1109 cm⁻¹ in gas-phase IR, which is in good agreement with literature data and VCI calculations. While the assignment of the ν_9 transition is unique in MI-IR (1051.4 cm⁻¹, Ne matrix), it is not straight-forward in gas-phase IR. Shimanouchi reports a band at 1048 cm⁻¹ with an uncertainty of 6–15 cm⁻¹. In accordance to Smith et al., we observe two well separated bands with similar intensity. The one of higher energy is somewhat split with peaks at 1062 cm⁻¹ and 1060 cm⁻¹ and nicely agrees with the VCI calculation. The other one at 1050.0 cm⁻¹, however, is in better agreement with the MI-IR experiments. The ν_{10} and ν_{17} fundamentals are observed in all experiments. Due to technical restrictions we were not able to record the region below 500 cm⁻¹ and can thus provide computational results only for the ν_{11} and ν_{18} fundamentals.

The region between 2740 cm⁻¹ and 2930 cm⁻¹ is dominated by a number of isolated bands of very weak intensity, which can mainly be assigned to combination bands and overtones. An exception is the band at 2920 cm⁻¹ (Ne matrix), which can be assigned to the ν_3 fundamental transition. Shimanouchi places this transition at 2915 cm⁻¹ with an error bar of 6–15 cm⁻¹, in accordance to the observation by Smith et al. In our gas-phase IR spectrum, the band is only indirectly observed and we would rather center the transition at around 2920 cm⁻¹, which is in good agreement with MI-IR experiments and VCI calculations. Considering also the other transitions in this region, the agreement of experimental and computed VCI(ae) results is excellent (cf. Table 3), while the computed VCI(fc) results tend to be slightly too low.

The region between 2940 cm^{-1} and 2956 cm^{-1} (Ne matrix) shows three bands of similar intensity (cf. 2955.1 cm^{-1} , 2947.2 cm^{-1} , and 2941.7 cm^{-1} in Fig. 2). In Ar matrix the band highest in frequency vanishes or is down-shifted, so that it overlays with one of the other two. Shimanouchi observes a band at 2941 cm^{-1} in the gas-phase and assigns it to ν_2 , but he reports an uncertainty of $6\text{--}15\text{ cm}^{-1}$ associated with this band. Smith et al. observe the same band. In contrast to that, we observe in our gas-phase IR spectrum a band at 2947.0 cm^{-1} . We reassign the ν_2 transition in the gas-phase and adopt it to the MI-IR spectra. However, the splitting in both Ne and Ar MI-IR remains intriguing. Considering the Ne MI-IR experiments, our VCI calculations for ν_2 allow for a more detailed discussion. The VCI(fc) calculation agrees nicely with the band at 2941.7 cm^{-1} , while the VCI(ae) calculation is in excellent agreement with the band at 2947.2 cm^{-1} . However, both calculations, i.e., with and without core-correlation, indicate a strong Fermi resonance of ν_2 with the overtone of ν_5 at 2914.7 cm^{-1} (Ne matrix). Although the VCI calculation including core-correlation is in much better agreement with the experimental value for $2\nu_5$ than that without core-correlation, it remains rather speculative to transfer this result to the Fermi partner. The situation becomes more complicated as the $\nu_4 + \nu_5$ combination band falls also in this region. According to our VCI calculations, this combination band should show up at 2958.3 cm^{-1} (fc) and 2957.3 cm^{-1} (ae). Consequently, the band highest in frequency can most likely be assigned to this combination band, but the assignment of ν_2 to one of the bands at 2941.7 cm^{-1} or 2947.2 cm^{-1} is not unique. Of course, the occurrence of these two bands may simply be due to matrix effects and thus both of them may belong to ν_2 . However, in gas-phase IR the different assignment in literature at 2941 cm^{-1} and by our observation at 2947 cm^{-1} basically implies the same problem. Thus, this may not be due to a matrix effect, but an inherent property of the vibrational structure.

The CH stretch region between 2985 cm^{-1} and 3010 cm^{-1} in MI-IR shows a rather complex structure, being dominated by three strong bands at 3000.9 cm^{-1} , 2996.8 cm^{-1} and 2990.5 cm^{-1} in Ne matrix (cf. Fig. 2). In all of these three bands, side bands of lower intensity occur, which are separated by about one wavenumber from the dominating bands. We reason this splitting as matrix effects that are specific to the Ne matrix. Besides these major bands, two features of lower intensity can be seen at about 2993.3 cm^{-1} and $3004.1/3005.7\text{ cm}^{-1}$. These bands are not as sharp as the dominating ones. In his gas-phase measurements Shimanouchi provides just one frequency to this region at 3003 cm^{-1} . He reports strong overlapping bands for ν_1 , ν_{12} and ν_{13} and, thus, gives essentially no detailed information about this region. Smith et al. report one A' fundamental at 3003 cm^{-1} and two A'' fundamentals at 3012 cm^{-1} and 2874 cm^{-1} . First of all, we can undoubtedly assign the ν_{13} fundamental transitions of A'' symmetry, observed in our gas-phase IR spectrum at 2964.8 cm^{-1} . Although there is some splitting in Ne matrix, the assignment of the ν_{13} transition is straight-forward in MI-IR (2966.3 cm^{-1} , Ne matrix). With that, we resolve the inconsistent assignment in literature (3003 cm^{-1} vs. 2874 cm^{-1}). In fact, Smith et al. observe a band at 2967 cm^{-1} and interpret it as an overtone. Problematic remains the assignment of the ν_1 and ν_{12} fundamentals. Our gas-phase experiments basically show just one strong and narrow band, and from this we would need to assign both transitions to one band (at 3000 cm^{-1}), similar as Shimanouchi. At this point, our MI-IR experiments provide most valuable information. As mentioned above, three major features with strong intensities can be observed in the Ne MI-IR spectrum (and in fact also in the Ar MI-IR spectrum, cf. Fig. 2). Combining these observations with the VCI calculations, we are in a position to resolve the involved CH stretch region. According to our VCI calculations including

core-correlation the strong band at 2996.8 cm^{-1} (Ne matrix) belongs to ν_1 , while the one at 3000.9 cm^{-1} (Ne matrix) can be assigned to ν_{12} . Our calculations indicate a very strong Fermi resonance of ν_1 with the overtone of ν_4 , which has been computed at 2990.2 cm^{-1} . The percentages of the VSCF configurations to these two states are shown in Table 4. This table clearly indicates that it is rather meaningless to assign one band to the fundamental and the other to the overtone. One would not expect such a strong intensity for an overtone as observed in our Ne matrix spectrum. However, the strong Fermi resonance allows for a distribution of the intensity of the fundamental between both states, which is further influenced by matrix effects. As a consequence, there is no unique assignment of ν_1 and $2\nu_4$ to the two observed bands in Ne matrix. However, we can certainly distinguish them from the bands at 3000.9 cm^{-1} and above, which must be assigned to the ν_{12} transition. This can be transferred to the gas-phase spectrum, where the band at 3000.0 cm^{-1} is assigned to the ν_{12} transition. Based on the assignment in the MI-IR spectra, the ν_1 transition must be expected also in gas-phase at a lower energy than the ν_{12} . Smith et al. report an A'' fundamental (which would correspond to ν_{12}) at 3012 cm^{-1} , being 9 cm^{-1} higher in energy than an A' fundamental (which would correspond to ν_1) at 3003 cm^{-1} . The energy difference between the ν_{12} and ν_1 agrees with the one we observe in Ar MI-IR. In fact, it also agrees with the difference observed in Ne MI-IR, when the before-mentioned Fermi resonance is assigned appropriately, with the band at 2990.2 cm^{-1} as ν_1 and the band at 2995.0 cm^{-1} as $2\nu_4$. Although we can agree with Smith et al. on the energy difference between ν_{12} and ν_1 we, still, do not agree with the assignment of the absolute energy to a band at 3012 cm^{-1} , as there is no hint for such a band neither in our MI-IR, nor in our gas-phase IR spectra. Furthermore, our VCI calculations do not predict the ν_{12} transition at such a high energy. Saur et al. [12] report the ν_1 transition at 2985 cm^{-1} , however, also in their spectrum this band is strongly overlapped by the R-branch of the ν_{12} transition and, thus, this assignment remains questionable. In order to understand the weak bands at about $3004.1/3005.7\text{ cm}^{-1}$ and 2993.3 cm^{-1} , we have performed additional calculations for combination bands of higher complexity and found a number of transitions, which fall into this region. Another possible explanation for the broad feature at $3004.1/3005.7\text{ cm}^{-1}$ would be the occurrence of oligomers in the matrix as the intensity of this band decreases significantly upon dilution.

4.4. Assignment of the fundamental vibrational transitions in the gas-phase and MI-IR spectrum of $\text{CD}_3\text{CD}_2\text{F}$

Both Shimanouchi [11] and Smith et al. [10] do not report any assignment for $\text{CD}_3\text{CD}_2\text{F}$. To the best of our knowledge, there is only one assignment by Saur et al. [12] available and this is used by McKean [16] to interpret his HA calculations. As the ν_1 , ν_{12} and ν_{13} transitions are not uniquely assigned in there, we decided to start from scratch and assign all observed bands in our MI-IR and gas-phase IR experiments based primarily on our VCI calculations. In general, our assignment is comparable to the one of Saur et al. [12], and we will only highlight the discrepancies for the sake of conciseness.

Table 4
Percentages of the configurations ν_1 and $2\nu_4$ to the VCI (ae) states at 2990.2 cm^{-1} and 2995.0 cm^{-1} .

	2990.2	2995.0
ν_1	31.2	28.4
$2\nu_4$	39.8	30.1

Table 5
Experimental and computed vibrational frequencies of CD₃CD₂F. All quantities are given in cm⁻¹.

Mode	Sym.	Experiment ^a			Calculation ^b				
		Gas	Ne	Ar	Harm.	fc-VCI	Δv _i (fc)	VCI(ae)	Δv _i (ae)
v ₁	A'	2242	2236.5	2235.5	2314.7	2236.3	6/0.2/0.8	2241.9	0/5.4/6.4
v ₂	A'	2127	2126.0	2127.4	2222.9	2125.6	1/0.4/1.8	2130.3	3/4.3/2.9
v ₃	A'	2083	2081.8	2078.7	2188.9	2080.1	3/1.7/1.4	2084.0	1/2.2/5.3
v ₄	A'	1204	1202.4	1197.5	1235.6	1203.3	1/0.9/5.8	1206.4	2/4.0/8.9
v ₅	A'	1127	1125.1	1120.3	1150.5	1126.4	1/1.3/6.1	1129.0	2/3.9/8.7
v ₆	A'	1075	1073.3	1070.3	1094.4	1072.9	2/0.4/2.6	1075.7	1/2.4/5.4
v ₇	A'	1058	1055.8	1053.4	1080.1	1055.3	3/0.5/1.9	1057.2	1/1.4/3.8
v ₈	A'	978	975.1	972.5	994.2	976.3	2/1.2/3.8	979.0	2/3.9/6.5
v ₉	A'	902	902.6	900.4	916.9	901.4	1/1.2/1.0	904.0	2/1.4/3.6
v ₁₀	A'	735	733.8	731.5	743.2	732.6	2/1.2/1.1	735.0	1/1.2/3.5
v ₁₁	A'	364 ^e	n.o. ^c	n.o. ^c	361.4	361.5		363.3	
v ₁₂	A''	2258	2256.7	2256.9	2328.7	2246.9	11/9.8/10.0	2253.0	5/3.7/3.9
v ₁₃	A''	2250	2248.4	2242.1	2308.4	2240.5	9/7.9/1.6	2245.8	4/2.6/3.7
v ₁₄	A''	1051	1050.5	1048.5	1071.4	1049.7	1/0.8/1.2	1051.4	0/0.9/2.9
v ₁₅	A''	n.o. ^d	988.0	984.7	1003.7	986.8	-1/1.2/2.1	989.4	-1/1.4/4.7
v ₁₆	A''	919	915.6	915.1	933.4	910.3	9/5.3/4.8	913.3	6/2.3/1.8
v ₁₇	A''	590 ^e	592.8	589.0	590.6	588.5	-4.3/0.5	591.0	-1/1.8/2.0
v ₁₈	A''	186 ^e	n.o. ^c	n.o. ^c	185.8	184.2		184.7	
						MAD	4/2.4/2.9		2/2.7/4.6
						MAX	11/9.8/10.0		2/5.4/8.9
2v ₅	A'				2301.0	2253.6		2258.8	
2v ₆	A'	2165.9	2164.0	2160.4	2188.8	2162.2		2167.9	
2v ₁₇	A'	1184.8	1186.4	1181.8	1181.2	1180.5		1185.4	
v ₄ + v ₁₄	A''	n.o.	2279.3	2272.2	2307.0	2257.9		2263.0	
v ₄ + v ₁₅	A''	n.o.	2177.1	2170.4	2239.3	2177.7		2181.2	
v ₄ + v ₈	A'	n.o.	2181.0	2174.1	2229.8	2179.3		2184.8	
v ₆ + v ₇	A'				2174.5	2127.4		2131.9	
v ₁₀ + v ₁₈	A''				929.0	923.1		926.0	
2v ₁₁ + v ₁₈	A''				908.6	918.6		922.6	

^a Vibrational frequencies measured in gas-phase, Ne matrix and Ar Matrix, this work.

^b Harmonic frequencies from fc-CCSD(T)-F12a/cc-pVTZ-F12 calculations. Anharmonic frequencies from VCI calculations including up to quintuple excitations, relying on a PES based on the frozen core (fc) approximation resp. on all electron (ae) correlation. Deviations Δv_i of the VCI(fc) and VCI(ae) frequencies calculated w.r.t. experimental Gas/Ne/Ar data.

^c Not observed, as the frequency is below the experimental spectral range.

^d Not observed, see text.

^e Taken from gas-phase reference [12], as cited in Ref. [16].

A straight-forward assignment is possible for the region up to 1230 cm⁻¹. We refer to Table 5 and do not go into detailed discussion for this region. However, some noteworthy observations shall be mentioned. The band which can be assigned to the v₄ transition shows a wild splitting pattern in the Ne matrix, while in Ar matrix it is only a little broadened. In the gas-phase, three bands are observed in this region, surrounded by prominent P- and R-branches. Although we can uniquely assign the v₄ transition, the residual two bands remain unclear. The v₈ transition was only indirectly observed in gas-phase IR experiments in between its P- and R-branch, while the v₁₅ transition is hidden behind the P-branch of the v₈ transition. The v₁₅ transition in gas-phase IR is also not reported by McKean. However, we undoubtedly find this transition in our Ne and Ar MI-IR experiments. Based on the good agreement with VCI calculation, we predict the v₁₅ transition in gas-phase IR at approximately 989 cm⁻¹. Due to its very low intensity, the v₁₇ transition is only partially observed in our MI-IR experiments and not observed at all in our gas-phase experiment. As we scanned only down to 500 cm⁻¹ we miss the observation of the v₁₈ transition.

The region from 2210 cm⁻¹ to 1230 cm⁻¹ comprises only two fundamentals. Considering the v₃ transition, in both Ne and Ar MI-IR two weak bands, split by approx. 10 cm⁻¹, are observed. Our VCI calculations do not predict any other transition in this region, hence, we suppose that this is a matrix effect. This assumption is somewhat enforced by our gas-phase IR experiments. While the assignment of the v₃ transition is not unique in the MI-IR spectra, in gas-phase we observe only one band that also perfectly agrees with the VCI calculation. More intriguing is the assignment

of the v₂ transition. In gas-phase it can be only indirectly derived at 2127 cm⁻¹, located in between its P- and R-branch. This agrees quite reasonably with the VCI calculated transition. Also in Ar MI-IR, a strong band is observed at 2127.6 cm⁻¹, which is in good agreement to gas-phase experiment and VCI calculations. However, a weaker band remains unassigned at 2117.3 cm⁻¹ in Ar MI-IR. In Ne MI-IR, a pattern of five bands is observed. The ones at 2131.2 cm⁻¹ and 2128.4 cm⁻¹ are of similar intensity, which decreases with dilution. We expect this to be some type of oligomerization within the Ne matrix. The split band at 2126.0/2124.8 cm⁻¹ can be assigned to the v₂ transition, as it is in good agreement with the other experiments and calculations. The weakest band of this pattern remains unassigned at 2121.4 cm⁻¹.

The CD-stretching region of CD₃CD₂F between 2290 cm⁻¹ and 2210 cm⁻¹ shows to be even more complicated than its already intriguing counterpart in the spectrum of CH₃CH₂F. There is one main reason for that. In the CH₃CH₂F spectrum, the v₁ and v₁₂ transitions are in a narrow region within 20 cm⁻¹ and the v₁₃ transition is nicely separated from them by approx. 30 cm⁻¹. In the CD₃CD₂F spectrum all those fundamentals conglomerate within a region of 35 cm⁻¹ and on top of that, the overtone 2v₅ and the combination band v₄ + v₁₄ can also be located in this region. The striking question is, which bands should be assigned to which transition. At this point, we can make use of the matrix-splitting patterns. Reconsidering the assignment of v₂ in Ne matrix, we observe five bands between 2140 cm⁻¹ and 2110 cm⁻¹ with a specific pattern. Actually, a very similar pattern is observed between 2253 cm⁻¹ and 2243 cm⁻¹. Visualization of the normal-modes shows, that the

Table 6Experimental and computed isotopic frequency shifts from CH₃CH₂F to CD₃CD₂F. All quantities are given in cm⁻¹.

Mode	Sym.	Experiment ^a			Calculation ^b		
		Gas	Ne	Ar	Harm.	VCI(fc)	VCI(ae)
ν_1	A'		-754.0	-752.2	-745.4	-747.2	-748.3
ν_2	A'	-820.4	-821.2	-822.5	-823.2	-817.0	-818.4
ν_3	A'	-836.8	-838.2	-842.0	-814.0	-838.2	-841.4
ν_4	A'	-286.8	-286.6	-288.1	-294.6	-285.0	-285.0
ν_5	A'	-338.9	-339.2	-340.8	-356.9	-336.0	-336.1
ν_6	A'	-322.0	-324.1	-324.7	-337.6	-322.8	-323.1
ν_7	A'		-315.5	-315.8	-322.4	-313.2	-314.8
ν_8	A'	-131.5	-133.5	-132.6	-138.0	-130.6	-131.1
ν_9	A'	-147.8	-148.8	-145.9	-167.6	-154.0	-154.8
ν_{10}	A'	-146.5	-145.2	-143.0	-152.2	-145.5	-145.7
ν_{11}	A'				-49.9	-49.5	-49.8
ν_{12}	A''	-742.0	-744.2	-748.4	-812.6	-746.5	-747.7
ν_{13}	A''	-715.3	-717.9	-731.0	-795.9	-722.3	-723.7
ν_{14}	A''	-397.6	-397.6	-396.2	-417.7	-395.3	-395.9
ν_{15}	A''		-288.7	-292.1	-303.9	-288.2	-289.4
ν_{16}	A''	-253.5	-257.3	-255.9	-262.3	-261.3	-261.2
ν_{17}	A''		-218.2	-218.7	-221.3	-217.2	-217.9
ν_{18}	A''				-65.7	-64.4	-64.3

^a Vibrational frequencies measured in gas-phase, Ne matrix and Ar Matrix, this work.^b Harmonic frequencies from fc-CCSD(T)-F12a/cc-pVTZ-F12 calculations. Anharmonic frequencies from VCI calculations including up to quintuple excitations, relying on a PES based on the frozen core (fc) approximation resp. on all electron (ae) correlation. Deviations $\Delta\nu_i$ of the VCI(fc) and VCI(ae) frequencies calculated w.r.t. experimental Gas/Ne/Ar data.

principle motion of the ν_{13} fundamental is the CH₂ asymmetric stretch and of the ν_2 fundamental the CH₂ symmetric stretch, both "located" at the fluoromethyl part. Hence, one may assume a similar matrix-splitting pattern for ν_{13} as for ν_2 , no matter the reasons for this splitting. Based on this assumption, the ν_{13} transition can be assigned to the band at 2248.4 cm⁻¹ in Ne matrix, being the most intense band within this matrix-splitting pattern. The good agreement with VCI calculations (2245.8 cm⁻¹) finally substantiates this assignment. In a similar fashion, we can assume that there must be a similar matrix-splitting pattern for ν_3 (observed between 2095 cm⁻¹ and 2075 cm⁻¹) and ν_1 (observed between 2243 cm⁻¹ and 2230 cm⁻¹), as the principle motion of the corresponding normal-modes is the CH₃ stretch for both ν_3 and ν_1 . For the ν_3 transition, two weak bands of almost same intensity split by 11 cm⁻¹ are observed. Based on our assumption of similar matrix-splittings, the ν_1 counterpart would be at 2242.3 cm⁻¹ and 2236.5 cm⁻¹, i.e., the two bands split by 5.9 cm⁻¹. Our VCI (ae) calculation predicts the transition at 2241.9 cm⁻¹, which is in good agreement with the higher one of those bands. However, for the sake of consistency we assign the ν_1 transition as the lower one of those bands (2236.5 cm⁻¹), as we also assigned the lower one in the case of ν_3 . Analogously for the Ar MI-IR experiments, based on the same assumption, we find the ν_{13} transition at 2242.1 cm⁻¹ and the ν_1 transition at 2235.5 cm⁻¹. Of course, we cannot make use of such arguments for the gas-phase experiments, as there is no matrix that could have comparable effect on two similar vibrational transitions. However, with the information derived from the two different MI-IR experiments, we are confident to assign in our gas-phase experiments the ν_{13} transition at 2249.7 cm⁻¹ and the ν_1 transition at 2241.7 cm⁻¹. Finally, the ν_{12} transition can be clearly distinguished from the other fundamentals, hence, undoubtedly assigned (Ne: 2256.7 cm⁻¹, Ar: 2256.9 cm⁻¹, gas: 2258.0 cm⁻¹).

4.5. Isotopic frequency shifts from gas-phase IR, MI-IR and VCI computations

When going from CH₃CH₂F to CD₃CD₂F, the fundamental vibrational transitions are expected to redshift towards lower frequencies. The isotopic shifts obtained from this work are listed in

Table 6. The experimental isotopic shifts in gas-phase IR and both Ne and Ar MI-IR are in excellent agreement to each other, except for the isotopic shift of the ν_{13} transition in Ar MI-IR which shows to be especially influenced by the Argon environment. In general, the spectral range of 4000 cm⁻¹ to 500 cm⁻¹ studied in this work, can be divided into two categories with systematically different isotopic shifts. The region below 1500 cm⁻¹ comprising the transitions ν_4 to ν_{10} and ν_{14} to ν_{17} shows isotopic shifts in between 100 to 400 cm⁻¹. The region above 1500 cm⁻¹ comprising the transitions ν_1 to ν_3 and ν_{12} , ν_{13} shows isotopic shifts in between 700 to 850 cm⁻¹. As one may comprehend from **Table 6**, the calculated isotopic shifts within the harmonic approximation are capable of reproducing this dissection into two categories. As the isotopic shifts from the harmonic approximation are qualitatively correct, they allow for an indirect assignment. That is, regions in the non-deuterated species' spectrum that are difficult to assign due to resonances between various CH stretch fundamentals and CH deformation overtones and combination bands, can be indirectly solved by transferring the assignment of the deuterated species' spectrum through isotopic frequency shifts. However, quantitatively the isotopic shifts from the harmonic approximation can extremely deviate from the experimentally observed. In the harmonic approximation, the isotopic shifts of the ν_4 , ν_6 and ν_{15} transitions are off by roughly 20 cm⁻¹; and the isotopic shifts of the ν_{12} , ν_{13} and ν_{14} transitions are off by 50 cm⁻¹ and more. In spite of such large deviations, an indirect assignment based on isotopic shifts from the harmonic approximation may not be blindly trusted. In contrast to that, both the VCI(ae) and VCI(fc) calculated isotopic shifts exhibit an excellent quantitative agreement with the isotopic shifts deduced from all experiments in this work, as can be nicely seen in **Table 6**. In fact, the VCI calculated frequencies are so accurate that the discussion on isotopic shifts can be seen as a validation of the assignment rather than a necessity for it.

5. Summary and conclusions

The mid infrared spectrum of fluoroethane and fluoroethane-d₅ has been revisited by means of gas-phase infrared experiments and extended by Neon and Argon matrix-isolation infrared (MI-IR) experiments. With the matrix-isolation technique, the mid infrared

spectrum of this hydrocarbon derivative has been resolved for the first time in a way that allows for a rigorous assignment of all fundamental vibrational transitions. This applies especially for the dissection of the ν_{12} , ν_{13} and ν_1 transitions in the CH resp. CD stretch region, which has not yet been fully understood in the literature. The final assignment of all transitions is made possible by *ab initio* calculations for the prediction of the anharmonic vibrational spectrum of fluoroethane. This has been achieved by extensive vibrational self-consistent field (VSCF) and configuration interaction (VCI) calculations on a 4-mode potential energy surface at CCSD(T)-F12 level of theory. It has been shown that a very good agreement between theory and experiment can be achieved if core-correlation is taken into account in the computation of the electronic structure. Vibrationally averaged structural parameters derived from this type of calculation are in very good agreement with experiment, too. This study of fluoroethane is an example par excellence for a class of small and volatile hydrocarbon derivatives, whose spectroscopic characterization in the atmosphere is of great relevance. We demonstrate that the interplay of high-resolution experimental MI-IR spectra and highly accurate computational prediction within the VSCF/VCI approach provides a route toward a rigorous characterization of such species.

Declaration of Competing Interest

The authors declare that they have no known competing financial interests or personal relationships that could have appeared to influence the work reported in this paper.

Acknowledgments

This research was supported in part by the bwHPC initiative and the bwHPC-C5 project provided through associated compute services of the JUSTUS HPC facility at the University of Ulm. bwHPC and bwHPC-C5 are funded by the Ministry of Science, Research and the Arts Baden-Württemberg (MWK). Financial support was provided by the Deutsche Forschungsgemeinschaft (DFG), project RA 656/20-1, and the Studienstiftung des Deutschen Volkes. We gratefully acknowledge support by the Austrian Science Fund FWF (project I1392 and project P30565) and the Austria Research Promotion Agency FFG (bridge project EARLYSNOW, 850689). M. P. would like to thank the FWF for a Lise Meitner postdoctoral fellowship (M-2005).

Appendix A. Supplementary material

Supplementary data associated with this article can be found, in the online version, at <https://doi.org/10.1016/j.jms.2019.111224>.

References

- [1] Handbook for the Montreal Protocol on Substances that Deplete the Ozone Layer, Thirteenth edition, United Nations Environment Programme. Ozone Secretariat, 2019. https://ozone.unep.org/sites/default/files/Handbooks/MP_Handbook_2019.pdf.
- [2] IPCC, 2013: Climate Change 2013: The Physical Science Basis. Contribution of Working Group I to the Fifth Assessment Report of the Intergovernmental Panel on Climate Change [Stocker, T.F., D. Qin, G.-K. Plattner, M. Tignor, S.K. Allen, J. Boschung, A. Nauels, Y. Xia, V. Bex and P.M. Midgley (eds.)]. Cambridge University Press, Cambridge, United Kingdom and New York, NY, USA, 1535 pp. The download link is: https://www.ipcc.ch/site/assets/uploads/2018/02/WG1AR5_all_final.pdf.
- [3] G.J.M. Velders, S.O. Andersen, J.S. Daniel, D.W. Fahey, M. McFarland, The importance of the Montreal Protocol in protecting climate, *Proc. Natl. Acad. Sci. U.S.A.* 104 (12) (2007) 4814–4819.
- [4] B. Xiang, P.K. Patra, S.A. Montzka, S.M. Miller, J.W. Elkins, F.L. Moore, E.L. Atlas, B.R. Miller, R.F. Weiss, R.G. Prinn, S.C. Wofsy, Global emissions of refrigerants HCFC-22 and HFC-134a: Unforeseen seasonal contributions, *Proc. Natl. Acad. Sci. U.S.A.* 111 (49) (2014) 17379–17384.
- [5] Kyoto Protocol to the United Nations Framework Convention on Climate Change, United Nations, 1998. <https://unfccc.int/resource/docs/convkp/kpeng.pdf>.
- [6] M. Mohanraj, S. Jayaraj, C. Muraleedharan, Environment friendly alternatives to halogenated refrigerants-A review, *Int. J. Greenh. Gas Cont.* 3 (1) (2009) 108–119.
- [7] Y. Xuan, G. Chen, Experimental study on HFC-161 mixture as an alternative refrigerant to R502, *Int. J. Refrig.* 28 (3) (2005) 436–441.
- [8] K.N. Kothale, S.D. Nimbalkar, Study of R-161 refrigerant as an Alternate Refrigerant to various other refrigerants, *Int. J. Curr. Eng. Technol.* 4 (4) (2016) 236–241.
- [9] D. Huppmann, J. Rogelj, E. Kriegler, V. Krey, K. Riahi, A new scenario resource for integrated 1.5 °C research, *Nat. Clim. Chang.* 8 (12) (2018) 1027–1030.
- [10] D.C. Smith, R. Saunders, J. Rud Nielsen, E. Ferguson, Infra-red and raman spectra of fluorinated ethanes. IV. The series CH₃-CH₃, CH₃-CH₃F, CH₃-CHF₂, and CH₃-CF₃, *J. Chem. Phys.* 20 (847) (1952).
- [11] T. Shimanouchi, NSRDS-NBS39. Tables of molecular vibrational frequencies, consolidated Volume I, *Nat. Stand. Ref. Data Ser., Nat. Bur. Stand. (U.S.)* (39) (1972) 164.
- [12] O. Saur, J. Travert, J. Saussey, J.-C. Lavalley, Étude des spectres d'absorption infrarouge du monofluoroéthane et de trois composés analogues deutériés: CH₃CD₂F, CD₃CH₂F, CD₃CD₂F, *J. Chim. Phys.* 72 (1975) 907–913.
- [13] D.C. McKean, CH stretching frequencies, bond lengths and strengths in halogenated ethylenes, *Spectrochim. Acta A Mol. Biomol. Spectrosc.* 31 (9–10) (1975) 1167–1186.
- [14] S. Pappasavva, K.H. Illinger, J.E. Kenny, Ab initio calculations on fluoroethanes: geometries, dipole moments, vibrational frequencies, and infrared intensities, *J. Phys. Chem.* 100 (24) (1996) 10100–10110.
- [15] D.C. McKean, Quantum-chemical studies of fluoroethanes: vibrational assignments, isolated CH stretching frequencies, valence force constants, and bond length relationships, *J. Phys. Chem. A* 104 (39) (2000) 8995–9008.
- [16] D.C. McKean, Quantum-chemical studies of ethyl fluoride: structure, scaled force fields and electrical properties, *J. Mol. Struct.* 642 (1–3) (2002) 25–39.
- [17] O. Gálvez, A. Zoermer, A. Loewenschuss, H. Grothe, A combined matrix isolation and ab initio study of bromine oxides, *J. Phys. Chem. A* 110 (20) (2006) 6472–6481.
- [18] J. Bernard, M. Seidl, I. Kohl, K.R. Liedl, E. Mayer, Ó. Gálvez, H. Grothe, T. Loerting, Spectroscopic observation of matrix-isolated carbonic acid trapped from the gas phase, *Angew. Chem. Int. Edit.* 50 (8) (2011) 1939–1943.
- [19] T.B. Adler, G. Knizia, H.-J. Werner, A simple and efficient CCSD(T)-F12 approximation, *J. Chem. Phys.* 127 (2007) 221106.
- [20] H.-J. Werner, G. Knizia, F.R. Manby, Explicitly correlated coupled cluster methods with pair-specific geminals, *Mol. Phys.* 109 (3) (2011) 407–417.
- [21] K.A. Peterson, T.B. Adler, H.-J. Werner, Systematically convergent basis sets for explicitly correlated wavefunctions: the atoms H, He, B–Ne, and Al–Ar, *J. Chem. Phys.* 128 (8) (2008) 084102.
- [22] G. Rauhut, G. Knizia, H. Werner, Accurate calculation of vibrational frequencies using explicitly correlated coupled-cluster theory, *J. Chem. Phys.* 130 (2009) 054105.
- [23] P. Meier, M. Neff, G. Rauhut, Accurate vibrational frequencies of borane and its isotopologues, *J. Chem. Theory Comput.* 7 (1) (2011) 148–152.
- [24] T.A. Ruden, T. Helgaker, P. Jørgensen, J. Olsen, Coupled-cluster connected quadruples and quintuples corrections to the harmonic vibrational frequencies and equilibrium bond distances of HF, N₂, F₂, and CO, *J. Chem. Phys.* 121 (12) (2004) 5874–5884.
- [25] J. Koput, Ab initio potential energy surface and vibration-rotation energy levels of beryllium monohydroxide, *J. Comput. Chem.* 38 (1) (2017) 37–43.
- [26] S. Carter, S.J. Culik, J.M. Bowman, Vibrational self-consistent field method for many-mode systems: a new approach and application to the vibrations of CO adsorbed on Cu(100), *J. Chem. Phys.* 107 (1997) 10458–10469.
- [27] B. Ziegler, G. Rauhut, Localized normal coordinates in accurate vibrational structure calculations: benchmarks for small molecules, *J. Chem. Theory Comput.* 15 (2019) 4187–4196.
- [28] K. Pflüger, M. Paulus, S. Jagiella, T. Burkert, G. Rauhut, Multi-level vibrational SCF calculations and FTIR measurements on Furazan, *Theor. Chem. Acc.* 114 (2005) 327–332.
- [29] K. Yagi, S. Hirata, K. Hirao, Multiresolution potential energy surfaces for vibrational state calculations, *Theor. Chim. Acta* 118 (2007) 681–691.
- [30] B. Ziegler, G. Rauhut, Efficient generation of sum-of-products representations of high-dimensional potential energy surfaces based on multimode expansions, *J. Chem. Phys.* 144 (2016) 114114.
- [31] K.M. Christoffel, J.M. Bowman, Investigations of self-consistent field, SCF CI and virtual state configuration-interaction vibrational energies for a model 3-mode system, *Chem. Phys. Lett.* 85 (1982) 220–224.
- [32] J.M. Bowman, K. Christoffel, F. Tobin, Application of SCF-CI theory to vibrational motion in polyatomic molecules, *J. Phys. Chem.* 83 (1979) 905–912.
- [33] M. Neff, G. Rauhut, Toward large scale vibrational configuration interaction calculations, *J. Chem. Phys.* 131 (2009) 124129.
- [34] M. Neff, T. Hrenar, D. Oschetzki, G. Rauhut, Convergence of vibrational angular momentum terms within the Watson hamiltonian, *J. Chem. Phys.* 134 (2011) 064105.
- [35] T. Petrenko, G. Rauhut, A new efficient method for the calculation of interior eigenpairs and its application to vibrational structure problems, *J. Chem. Phys.* 146 (2017) 124101.

- [36] L. Nygaard, A revised structure of ethyl fluoride, *Spectrochim. Acta* 22 (1966) 1261–1266.
- [37] B. Beagley, M.O. Jones, P. Yavari, Gas phase electron diffraction studies of the molecular structures of pentafluoroethane, C_2F_5H , and monofluoroethane, C_2H_5F , *J. Mol. Struct.* 71 (1981) 203–208.
- [38] G. Czako, E. Matyus, A.G. Csaszar, Bridging theory with experiment: a benchmark study of thermally averaged structural and effective spectroscopic parameters of the water molecule, *J. Phys. Chem. A* 113 (43) (2009) 11665–11678.
- [39] J.K.G. Watson, Simplification of molecular vibration-rotation hamiltonian, *Mol. Phys.* 15 (1968) 479–490.
- [40] G. Rauhut, Anharmonic Franck-Condon factors for the $\bar{X}^2B_1 \rightarrow \bar{X}^1A_1$ photoionization of ketene, *J. Phys. Chem. A* 119 (2015) 10264–10271.